



*Supplement of*

## **Multi-model ensemble projection of the global dust cycle by the end of 21st century using the Coupled Model Intercomparison Project version 6 data**

**Yuan Zhao et al.**

*Correspondence to:* Xu Yue (yuexu@nuist.edu.cn)

The copyright of individual parts of the supplement might differ from the article licence.

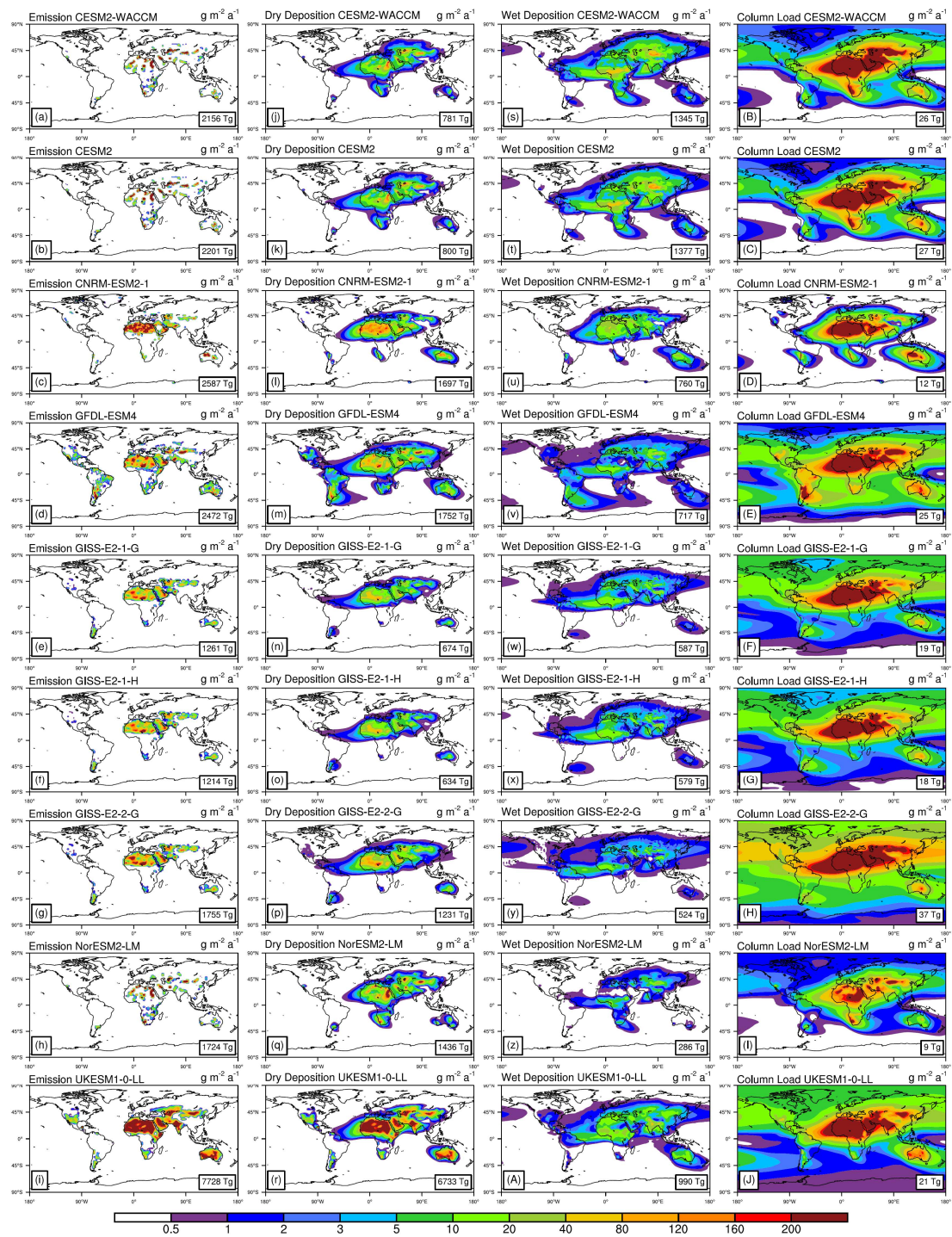


**Figure S1.** Dust emission and deposition of each selected model used in analyses at present day (2005-2014). Please notice that the median values in Fig. 4 are derived as the global total of gridded median results from CMIP6 models, and are different from the median values of the global total from CMIP6 models shown above.

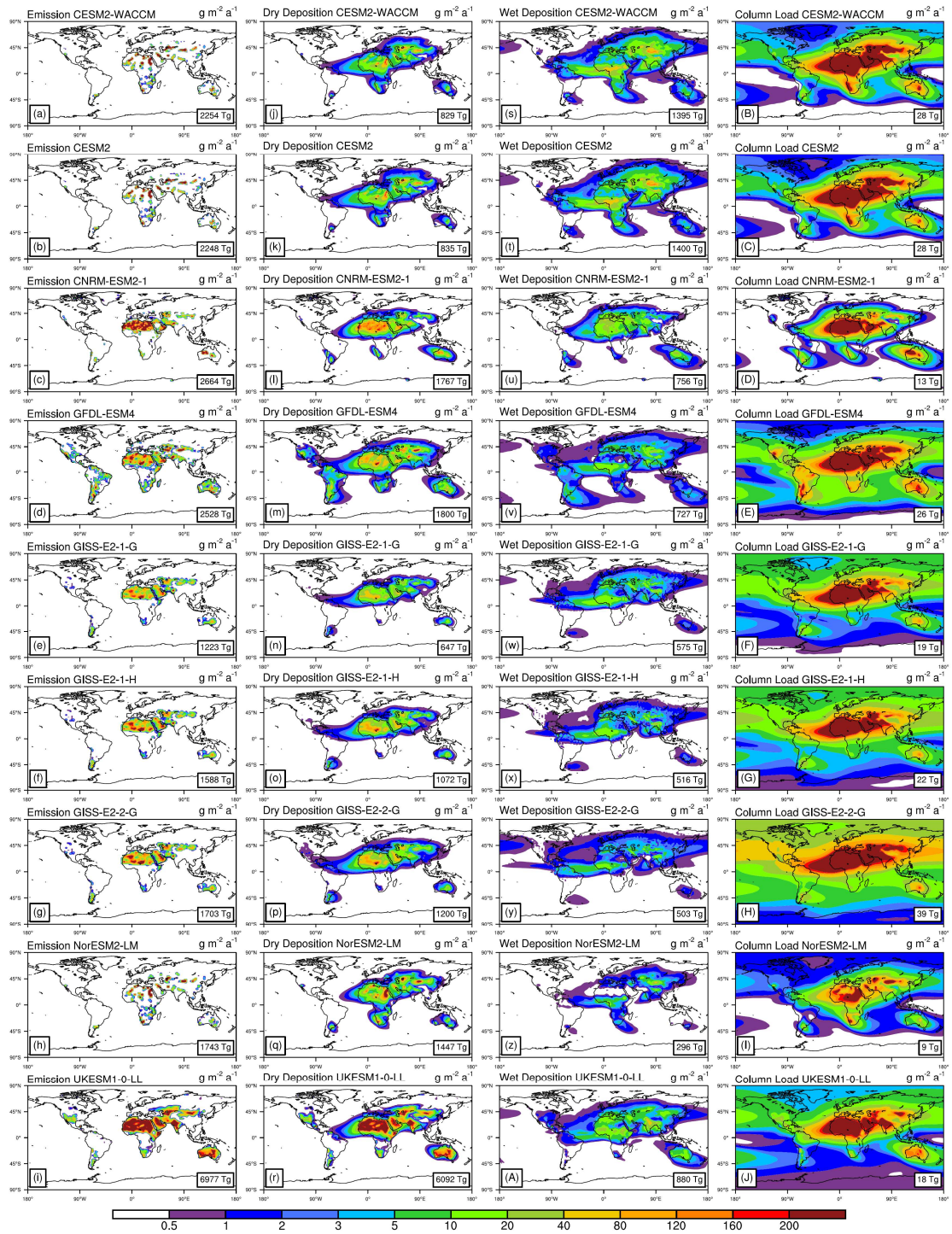


Figure S2. The same as Fig. S1 but in SSP1-2.6 scenario (2090-2099).



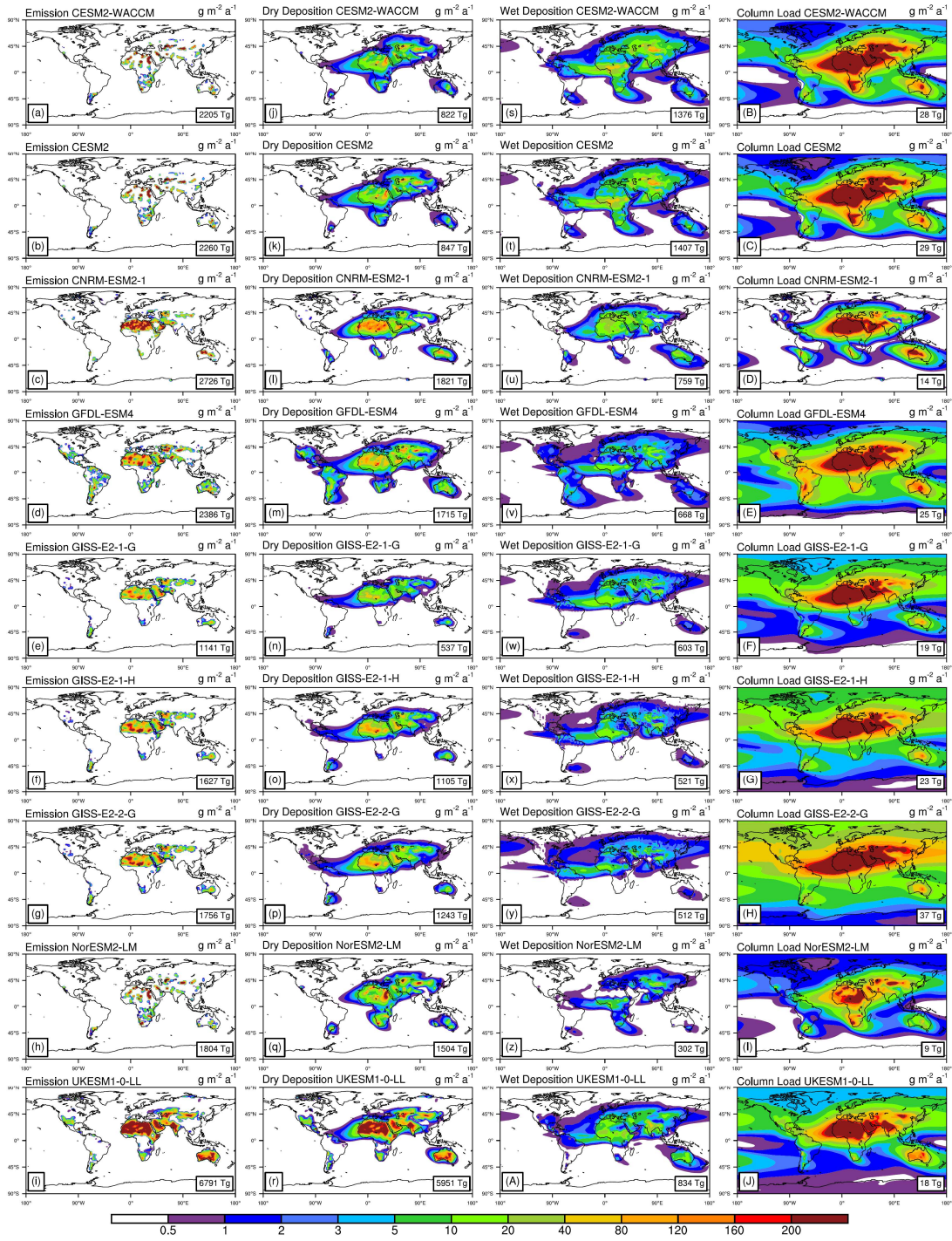


Figure S3. The same as Fig. S1 but in SSP2-4.5 scenario (2090-2099).



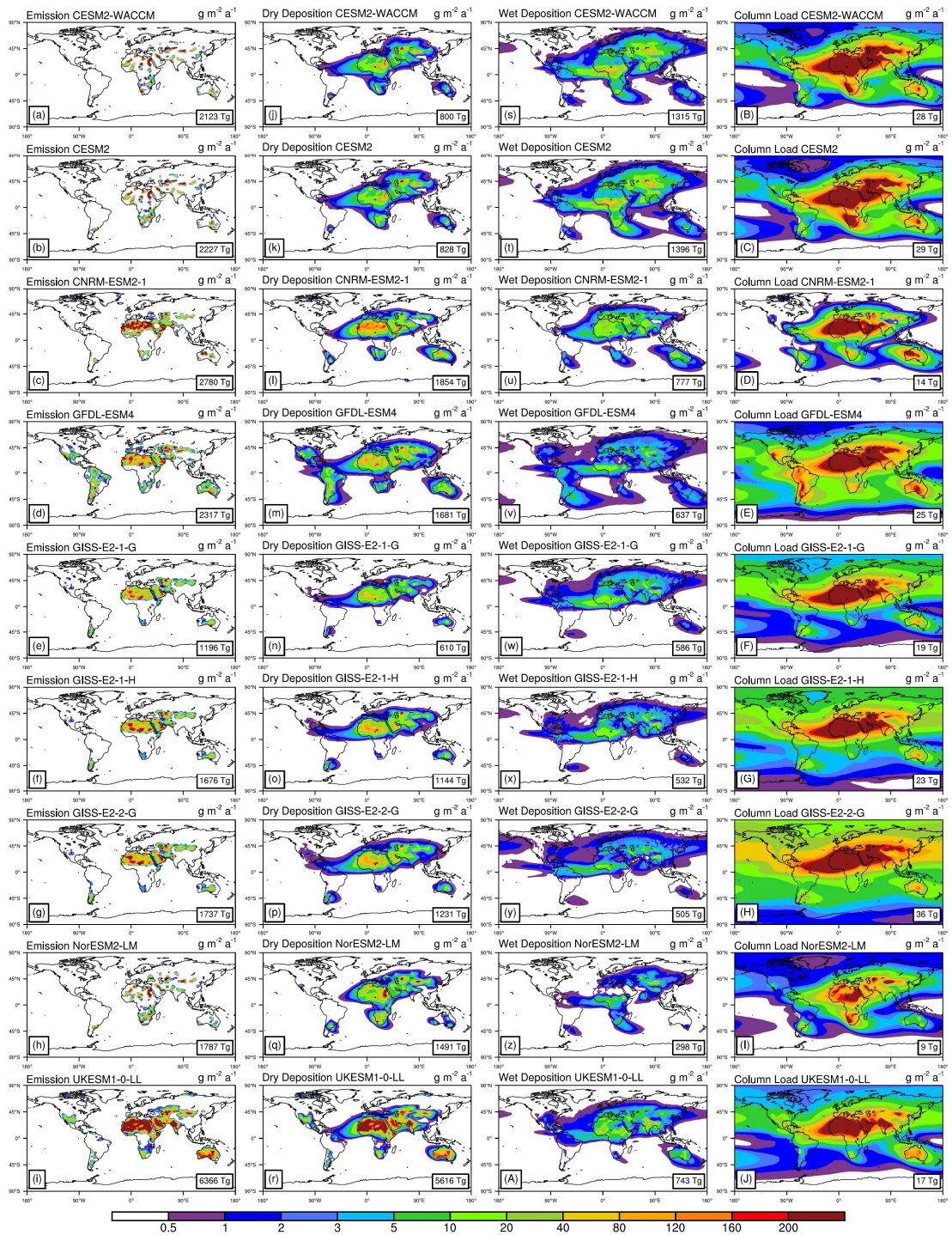


Figure S4. The same as Fig. S1 but in SSP3-7.0 scenario (2090-2099).

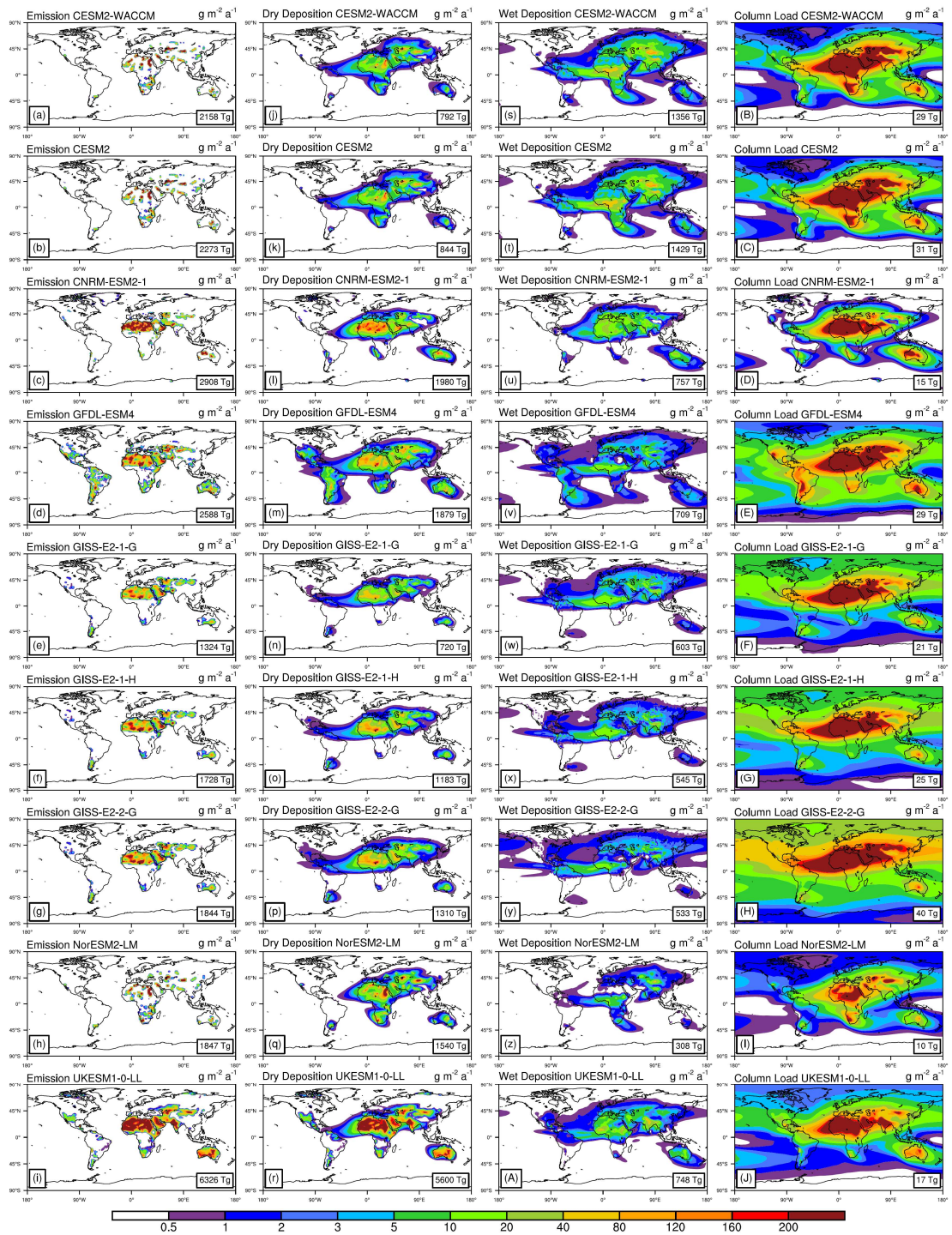
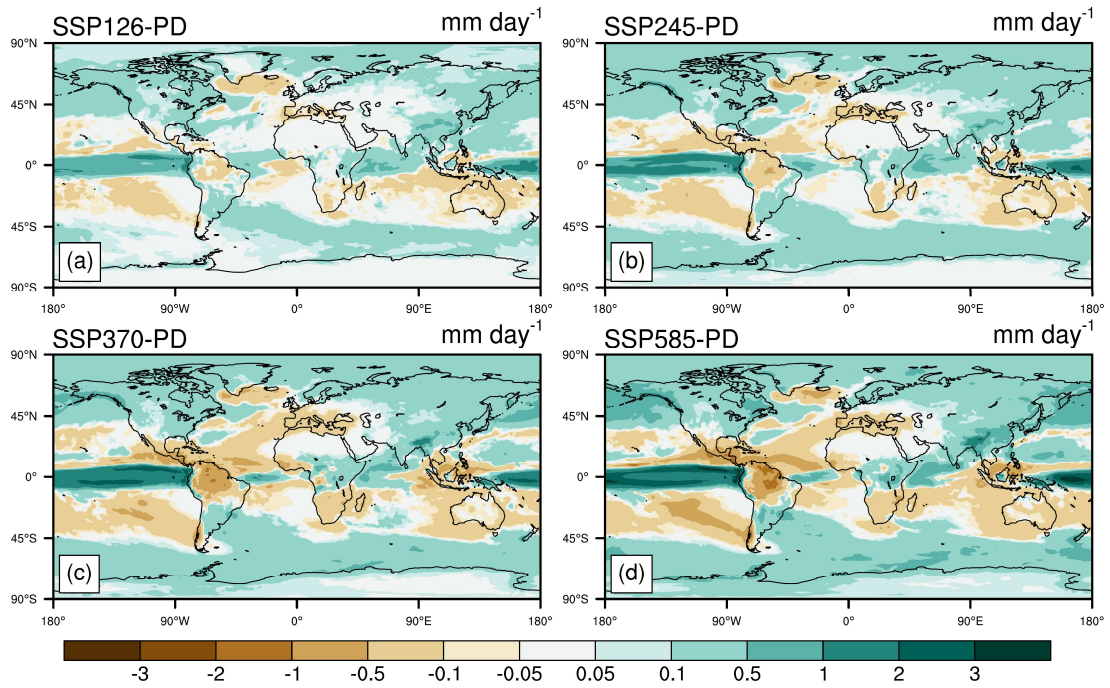


Figure S5. The same as Fig. S1 but in SSP5-8.5 scenario (2090-2099).





**Figure S6.** Multi-model ensemble projection of the changes in precipitation by the end of 21<sup>st</sup> century (2090-2099) relative to present day (2005-2014) under four different anthropogenic emission scenarios. Precipitation data from the nine selected climate models (Table 1) are used in the analyses.



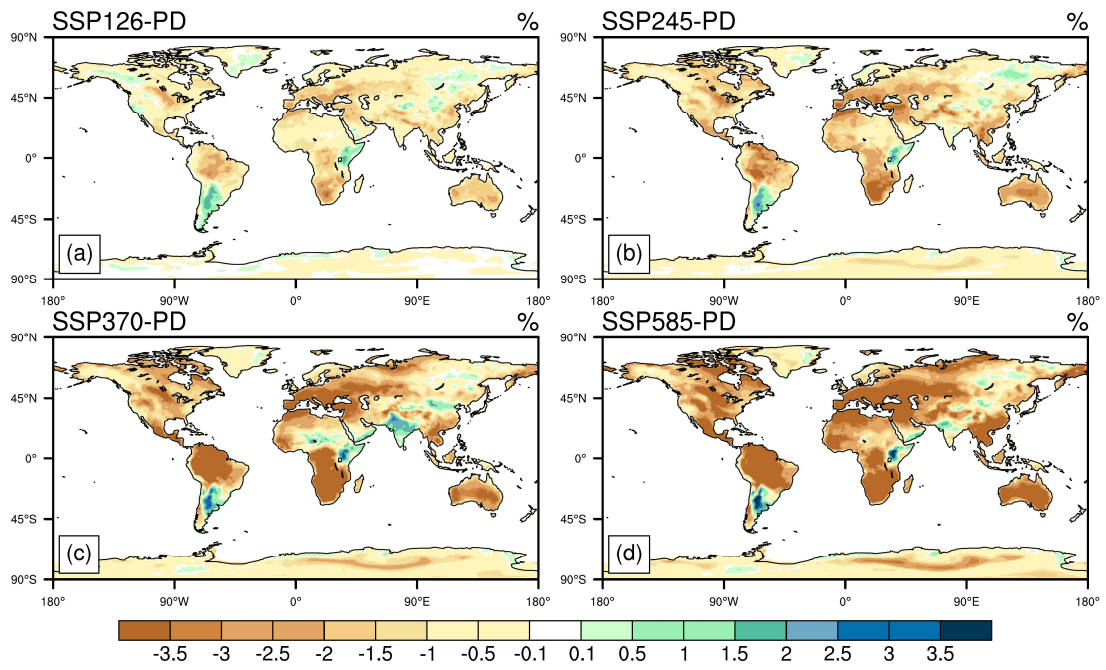


**Figure S7.** The same as Fig. S6 but for changes in relative humidity.

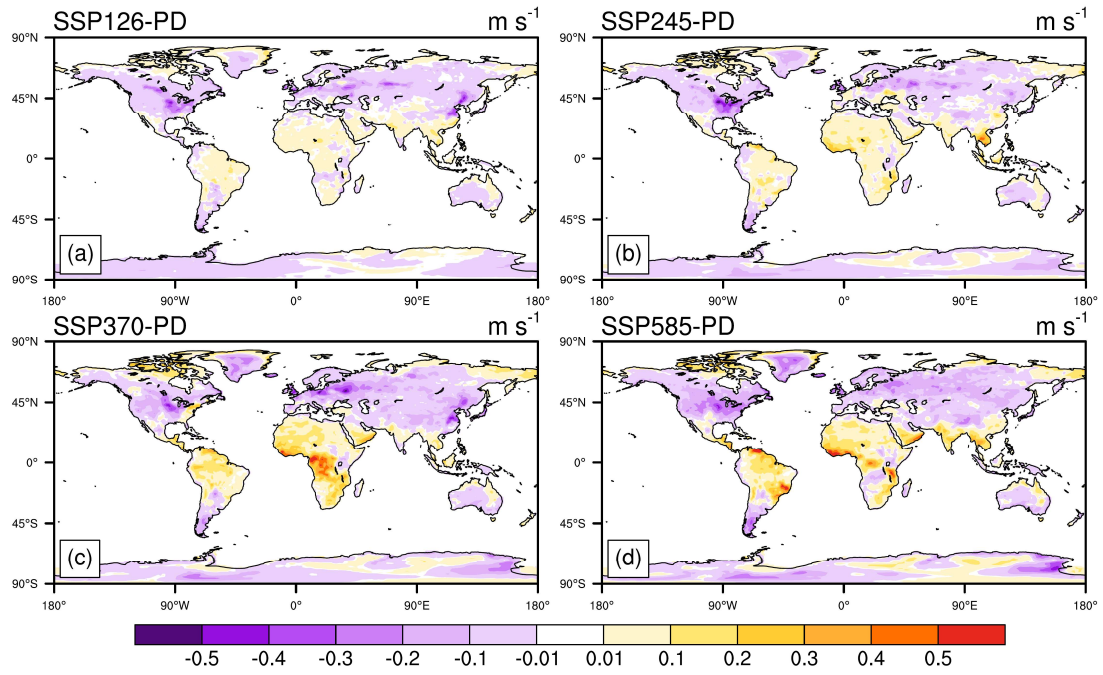


**Figure S8.** The same as Fig. S6 but for changes in surface wind speed.

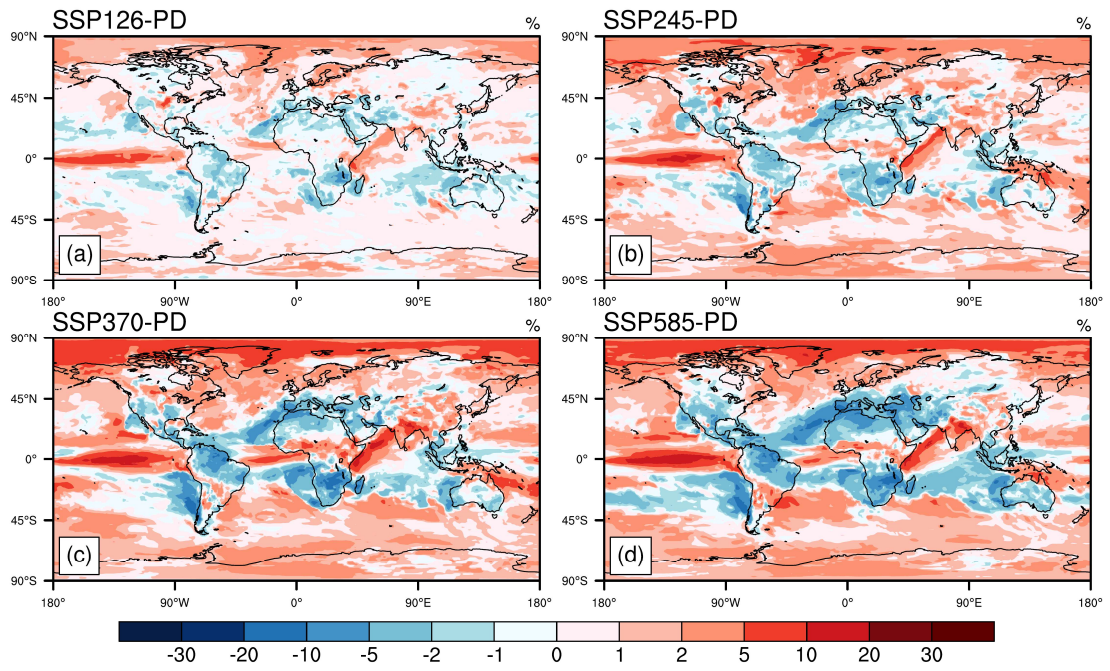


**Figure S9.** The same as Fig. S6 but for changes in the ratio of wet to total deposition.



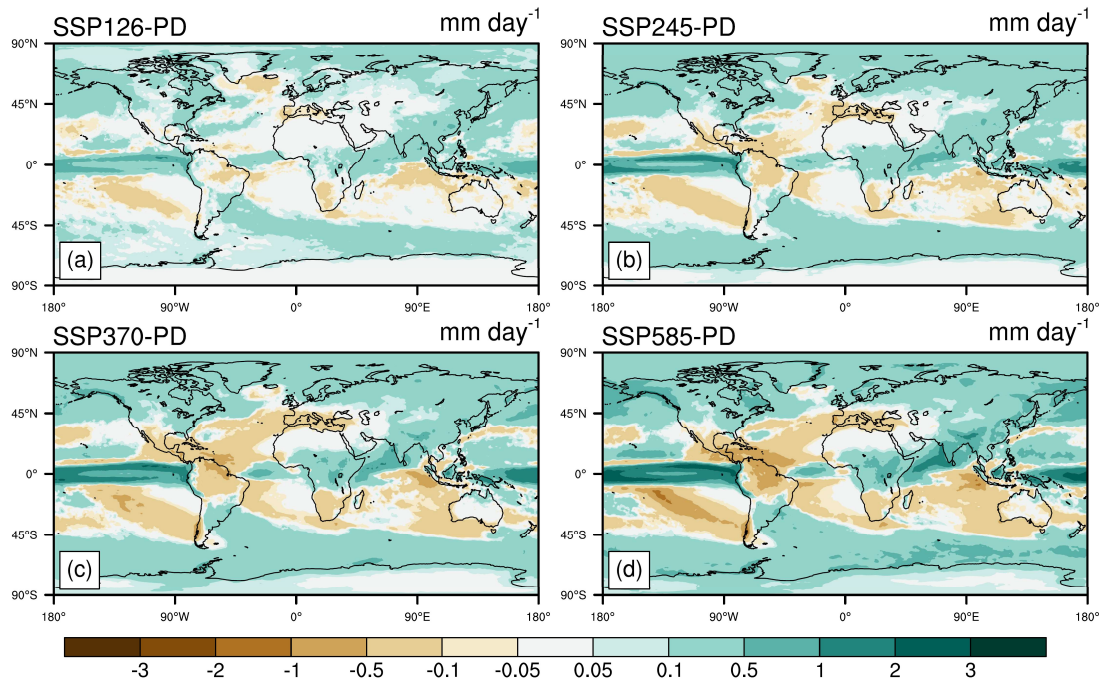


**Figure S10.** Multi-model ensemble projection of the changes in precipitation by the end of 21<sup>st</sup> century (2090-2099) relative to present day (2005-2014) under four different anthropogenic emission scenarios using all climate models in Table S7.

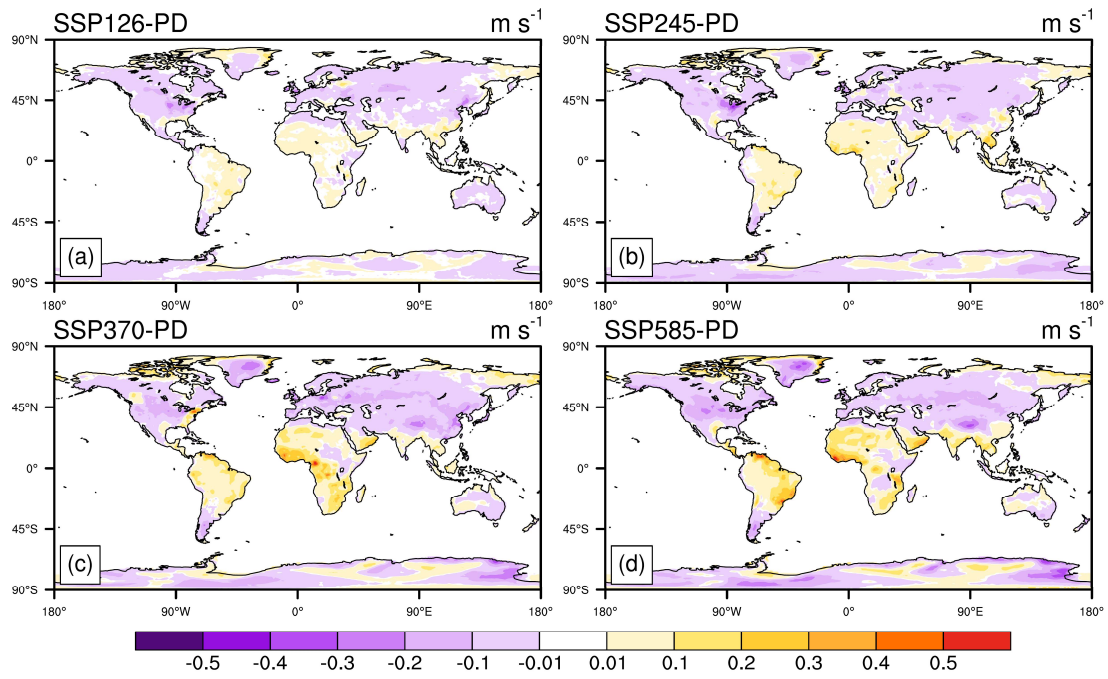


**Figure S11.** The same as Fig. S10 but for changes in surface wind speed.

**Table S1.** All ensemble runs of each available CMIP6 model for dust projection under different scenarios. The unused data are crossed out with a black line. The last access of the data information was on April 20<sup>th</sup>, 2023.

Experiment ID	Historical			
	emidust	drydust	wetdust	mmdrust
Model (# of runs)	Variant Label	Variant Label	Variant Label	Variant Label
CESM2 (11)	r[1-11]i1p1f1	r[1-11]i1p1f1	r[1-11]i1p1f1	r[1-11]i1p1f1
CESM2-WACCM (3)	r[1-3]i1p1f1	r[1-3]i1p1f1	r[1-3]i1p1f1	r[1-3]i1p1f1
CNRM-ESM2-1 (3)	r[1-3]i1f1p2 <del>r[4-5]i1f1p2</del> <del>r[8-11]i1p1f2</del>	r[1-3]i1f1p2 <del>r[4-5]i1f1p2</del> <del>r[8-11]i1p1f2</del>	r[1-3]i1f1p2 <del>r[4-5]i1f1p2</del> <del>r[8-11]i1p1f2</del>	r[1-3]i1p1f2
GFDL-ESM4 (1)	r1i1p1f1	r1i1p1f1	r1i1p1f1	r1i1p1f1
NorESM2-LM (1)	r1i1p1f1 <del>r[2-3]i1p1f1</del>	r1i1p1f1	r1i1p1f1	r1i1p1f1 <del>r[2-3]i1p1f1</del>
UKESM1-0-LL (3)	r[1-3]i1p1f2 <del>r[4-19]i1p1f2</del>	r[1-3]i1p1f2	r[1-3]i1p1f2	r[1-3]i1p1f2 <del>r[4-19]i1p1f2</del>
INM-CM4-8 (1)	r1i1p1f1	r1i1p1f1	r1i1p1f1	r1i1p1f1
INM-CM5-0 (10)	r[1-10]i1p1f1	r[1-10]i1p1f1	r[1-10]i1p1f1	r[1-10]i1p1f1
MIROC6 (10)	r[1-10]i1p1f1	r[1-10]i1p1f1	r[1-10]i1p1f1	r[1-10]i1p1f1
MIROC-ES2L (31)	r[1-30]i1p1f2 r1i1000p1f2	r[1-30]i1p1f2 r1i1000p1f2	r[1-30]i1p1f2 r1i1000p1f2	r[1-30]i1p1f2 r1i1000p1f2
MRI-ESM2-0 (12)	r[1-10]i1p1f1 r1i2p1f1 r1i1000p1f1	r[1-10]i1p1f1 r1i2p1f1 r1i1000p1f1	r[1-10]i1p1f1 r1i2p1f1 r1i1000p1f1	r[1-10]i1p1f1 r1i2p1f1 r1i1000p1f1
GISS-E2-1-G (19)	r[1-10]i1p3f1 r[1-4]i1p5f1 r[6-10]i1p5f1	r[1-10]i1p3f1 r[1-4]i1p5f1 r[6-10]i1p5f1	r[1-10]i1p3f1 r[1-4]i1p5f1 r[6-10]i1p5f1	r[1-10]i1p3f1 r[1-4]i1p5f1 r[6-10]i1p5f1
GISS-E2-1-H (10)	r[1-5]i1p3f1 r[1-5]i1p5f1	r[1-5]i1p3f1 r[1-5]i1p5f1	r[1-5]i1p3f1 r[1-5]i1p5f1	r[1-5]i1p3f1 r[1-5]i1p5f1
GISS-E2-2-G (5)	r[1-5]i1p3f1	r[1-5]i1p3f1	r[1-5]i1p3f1	r[1-5]i1p3f1
Experiment ID	ssp126			
Variable	emidust	drydust	wetdust	mmdrust
Model (# of runs)	Variant Label	Variant Label	Variant Label	Variant Label
CESM2 (3)	r4i1p1f1 r10i1p1f1 r11i1p1f1	r4i1p1f1 r10i1p1f1 r11i1p1f1	r4i1p1f1 r10i1p1f1 r11i1p1f1	r4i1p1f1 r10i1p1f1 r11i1p1f1
CESM2-WACCM (1)	r1i1p1f1	r1i1p1f1	r1i1p1f1	r1i1p1f1
CNRM-ESM2-1	r[1-5]i1p1f2	r[1-5]i1p1f2	r[1-5]i1p1f2	r[1-5]i1p1f2



(5)				
GFDL-ESM4 (1)	r1ilp1fl	r1ilp1fl	r1ilp1fl	r1ilp1fl
NorESM2-LM (1)	r1ilp1fl	r1ilp1fl	r1ilp1fl	r1ilp1fl
UKESM1-0-LL (5)	r[1-4]ilp1f2 r8ilp1f2 <del>r[5-7]ilp1f2</del> <del>r[9-19]ilp1f2</del>	r[1-4]ilp1f2 r8ilp1f2 <del>r[5-7]ilp1f2</del> <del>r[9-19]ilp1f2</del>	r[1-4]ilp1f2 r8ilp1f2 <del>r[5-7]ilp1f2</del> <del>r[9-19]ilp1f2</del>	r[1-4]ilp1f2 r8ilp1f2 <del>r[5-7]ilp1f2</del> <del>r[9-19]ilp1f2</del>
INM-CM4-8 (1)	r1ilp1fl	r1ilp1fl	r1ilp1fl	r1ilp1fl
INM-CM5-0 (1)	r1ilp1fl	r1ilp1fl	r1ilp1fl	r1ilp1fl
MIROC6 (3)	r[1-3]ilp1fl	r[1-3]ilp1fl	r[1-3]ilp1fl	r[1-3]ilp1fl
MIROC-ES2L (10)	r[1-10]ilp1f2	r[1-10]ilp1f2	r[1-10]ilp1f2	r[1-10]ilp1f2
MRI-ESM2-0 (5)	r[1-5]ilp1fl	r[1-5]ilp1fl	r[1-5]ilp1fl	r[1-5]ilp1fl
GISS-E2-1-G (10)	r[1-5]ilp3fl r[1-5]ilp5fl	r[1-5]ilp3fl r[1-5]ilp5fl	r[1-5]ilp3fl r[1-5]ilp5fl	r[1-5]ilp3fl r[1-5]ilp5fl
GISS-E2-1-H (5)	r[1-5]ilp3fl	r[1-5]ilp3fl	r[1-5]ilp3fl	r[1-5]ilp3fl
GISS-E2-2-G (5)	r[1-5]ilp3fl	r[1-5]ilp3fl	r[1-5]ilp3fl	r[1-5]ilp3fl
Experiment ID	ssp245			
Variable	emidust	drydust	wetdust	mmdust
Model (# of runs)	Variant Label	Variant Label	Variant Label	Variant Label
CESM2 (3)	r4ilp1fl r10ilp1fl r11ilp1fl	r4ilp1fl r10ilp1fl r11ilp1fl	r4ilp1fl r10ilp1fl r11ilp1fl	r4ilp1fl r10ilp1fl r11ilp1fl
CESM2-WACCM (5)	r[1-5]ilp1fl	r[1-5]ilp1fl	r[1-5]ilp1fl	r[1-5]ilp1fl
CNRM-ESM2-1 (10)	r[1-10]ilp1f2	r[1-10]ilp1f2	r[1-10]ilp1f2	r[1-10]ilp1f2
GFDL-ESM4 (1)	r1ilp1fl	r1ilp1fl	r1ilp1fl	r1ilp1fl
NorESM2-LM (13)	r[1-3]ilp1fl r[1-10]ilp1f2	r[1-3]ilp1fl r[1-10]ilp1f2	r[1-3]ilp1fl r[1-10]ilp1f2	r[1-3]ilp1fl r[1-10]ilp1f2
UKESM1-0-LL (5)	r[1-4]ilp1f2 r8ilp1f2 <del>r[13-15]ilp1f2</del>	r[1-4]ilp1f2 r8ilp1f2 <del>r[13-15]ilp1f2</del>	r[1-4]ilp1f2 r8ilp1f2 <del>r[13-15]ilp1f2</del>	r[1-4]ilp1f2 r8ilp1f2 <del>r[13-15]ilp1f2</del>
INM-CM4-8 (1)	r1ilp1fl	r1ilp1fl	r1ilp1fl	r1ilp1fl
INM-CM5-0 (1)	r1ilp1fl	r1ilp1fl	r1ilp1fl	r1ilp1fl
MIROC6 (3)	r[1-3]ilp1fl	r[1-3]ilp1fl	r[1-3]ilp1fl	r[1-3]ilp1fl
MIROC-ES2L (30)	r[1-30]ilp1f2	r[1-30]ilp1f2	r[1-30]ilp1f2	r[1-30]ilp1f2
MRI-ESM2-0 (10)	r[1-5]ilp1fl r[1-5]i3p1fl	r[1-5]ilp1fl r[1-5]i3p1fl	r[1-5]ilp1fl r[1-5]i3p1fl	r[1-5]ilp1fl r[1-5]i3p1fl
GISS-E2-1-G (25)	r[1-5]ilp3fl r[1-10]ilp5fl	r[1-5]ilp3fl r[1-10]ilp5fl	r[1-5]ilp3fl r[1-10]ilp5fl	r[1-5]ilp3fl r[1-10]ilp5fl

	r[1-10]i1p5f2	r[1-10]i1p5f2	r[1-10]i1p5f2	r[1-10]i1p5f2
GISS-E2-1-H (5)	r[1-5]i1p3f1	r[1-5]i1p3f1	r[1-5]i1p3f1	r[1-5]i1p3f1
GISS-E2-2-G (5)	r[1-5]i1p3f1	r[1-5]i1p3f1	r[1-5]i1p3f1	r[1-5]i1p3f1
Experiment ID	ssp370			
Variable	emidust	drydust	wetdust	mmdrust
Model (# of runs)	Variant Label	Variant Label	Variant Label	Variant Label
CESM2 (3)	r4i1p1f1 r10i1p1f1 r11i1p1f1	r4i1p1f1 r10i1p1f1 r11i1p1f1	r4i1p1f1 r10i1p1f1 r11i1p1f1	r4i1p1f1 r10i1p1f1 r11i1p1f1
CESM2-WACCM (3)	r[1-3]i1p1f1	r[1-3]i1p1f1	r[1-3]i1p1f1	r[1-3]i1p1f1
CNRM-ESM2-1 (5)	r[1-5]i1p1f2	r[1-5]i1p1f2	r[1-5]i1p1f2	r[1-5]i1p1f2
GFDL-ESM4 (1)	r1i1p1f1	r1i1p1f1	r1i1p1f1	r1i1p1f1
NorESM2-LM (1)	r1i1p1f1 <del>r[2-3]i1p1f1</del>	r1i1p1f1	r1i1p1f1	r1i1p1f1 <del>r[2-3]i1p1f1</del>
UKESM1-0-LL (3)	r[1-3]i1p1f2 <del>r[4-8]i1p1f2</del> <del>r[13-16]i1p1f2</del> r19i1p1f2	r[1-3]i1p1f2	r[1-3]i1p1f2	r[1-3]i1p1f2 <del>r[4-8]i1p1f2</del> <del>r[13-16]i1p1f2</del> r19i1p1f2
INM-CM4-8 (1)	r1i1p1f1	r1i1p1f1	r1i1p1f1	r1i1p1f1
INM-CM5-0 (5)	r[1-5]i1p1f1	r[1-5]i1p1f1	r[1-5]i1p1f1	r[1-5]i1p1f1
MIROC6 (3)	r[1-3]i1p1f1	r[1-3]i1p1f1	r[1-3]i1p1f1	r[1-3]i1p1f1
MIROC-ES2L (10)	r[1-10]i1p1f2	r[1-10]i1p1f2	r[1-10]i1p1f2	r[1-10]i1p1f2
MRI-ESM2-0 (5)	r[1-5]i1p1f1	r[1-5]i1p1f1	r[1-5]i1p1f1	r[1-5]i1p1f1
GISS-E2-1-G (17)	r[1-3]i1p3f2 r[1-4]i1p3f1 r[1-10]i1p5f1	r[1-3]i1p3f2 r[1-4]i1p3f1 r[1-10]i1p5f1	r[1-3]i1p3f2 r[1-4]i1p3f1 r[1-10]i1p5f1	r[1-3]i1p3f2 r[1-4]i1p3f1 r[1-10]i1p5f1
GISS-E2-1-H (1)	r1i1p3f1	r1i1p3f1	r1i1p3f1	r1i1p3f1
GISS-E2-2-G (5)	r[1-5]i1p3f1	r[1-5]i1p3f1	r[1-5]i1p3f1	r[1-5]i1p3f1
Experiment ID	ssp585			
Variable	emidust	drydust	wetdust	mmdrust
Model (# of runs)	Variant Label	Variant Label	Variant Label	Variant Label
CESM2 (3)	r4i1p1f1 r10i1p1f1 r11i1p1f1	r4i1p1f1 r10i1p1f1 r11i1p1f1	r4i1p1f1 r10i1p1f1 r11i1p1f1	r4i1p1f1 r10i1p1f1 r11i1p1f1
CESM2-WACCM (5)	r[1-5]i1p1f1	r[1-5]i1p1f1	r[1-5]i1p1f1	r[1-5]i1p1f1
CNRM-ESM2-1 (5)	r[1-5]i1p1f2	r[1-5]i1p1f1	r[1-5]i1p1f1	r[1-5]i1p1f2
GFDL-ESM4 (1)	r1i1p1f1	r1i1p1f1	r1i1p1f1	r1i1p1f1

NorESM2-LM (1)	r1i1p1f1	r1i1p1f1	r1i1p1f1	r1i1p1f1
UKESM1-0-LL (4)	r[1-4]i1p1f2 <del>r8i1p1f2</del> <del>r[13-15]i1p1f2</del>	r[1-4]i1p1f2	r[1-4]i1p1f2	r[1-4]i1p1f2 <del>r8i1p1f2</del> <del>r[13-15]i1p1f2</del>
INM-CM4-8 (1)	r1i1p1f1	r1i1p1f1	r1i1p1f1	r1i1p1f1
INM-CM5-0 (1)	r1i1p1f1	r1i1p1f1	r1i1p1f1	r1i1p1f1
MIROC6 (3)	r[1-3]i1p1f1	r[1-3]i1p1f1	r[1-3]i1p1f1	r[1-3]i1p1f1
MIROC-ES2L (10)	r[1-10]i1p1f2	r[1-10]i1p1f2	r[1-10]i1p1f2	r[1-10]i1p1f2
MRI-ESM2-0 (6)	r[1-5]i1p1f1 r1i2p1f1	r[1-5]i1p1f1 r1i2p1f1	r[1-5]i1p1f1 r1i2p1f1	r[1-5]i1p1f1 r1i2p1f1
GISS-E2-1-G (10)	r[1-5]i1p3f1 r[1-5]i1p5f1	r[1-5]i1p3f1 r[1-5]i1p5f1	r[1-5]i1p3f1 r[1-5]i1p5f1	r[1-5]i1p3f1 r[1-5]i1p5f1
GISS-E2-1-H (5)	r[1-5]i1p3f1	r[1-5]i1p3f1	r[1-5]i1p3f1	r[1-5]i1p3f1
GISS-E2-2-G (5)	r[1-5]i1p3f1	r[1-5]i1p3f1	r[1-5]i1p3f1	r[1-5]i1p3f1
Experiment ID	historical			
Variable	hurs	pr	sfcWind	
Model (# of runs)	Variant Label	Variant Label	Variant Label	
CESM2 (11)	r[1-11]i1p1f1	r[1-11]i1p1f1	r[1-11]i1p1f1	
CESM2-WACCM (3)	r[1-3]i1p1f1	r[1-3]i1p1f1	r[1-3]i1p1f1	
CNRM-ESM2-1 (10)	r[1-10]i1p1f2 <del>r11i1p1f2</del>	r[1-10]i1p1f2 <del>r11i1p1f2</del>	r[1-10]i1p1f2	
GFDL-ESM4 (1)	r1i1p1f1 <del>r[2-3]i1p1f1</del>	r1i1p1f1 <del>r[2-3]i1p1f1</del>	r1i1p1f1	
NorESM2-LM (3)	r[1-3]i1p1f1	r[1-3]i1p1f1	r[1-3]i1p1f1	
UKESM1-0-LL (19)	r[1-4]i1p1f2 r[5-7]i1p1f3 r[8-19]i1p1f2	r[1-4]i1p1f2 r[5-7]i1p1f3 r[8-19]i1p1f2	r[1-4]i1p1f2 r[5-7]i1p1f3 r[8-19]i1p1f2	
INM-CM4-8 (1)	r1i1p1f1	r1i1p1f1	r1i1p1f1	
INM-CM5-0 (10)	r[1-10]i1p1f1	r[1-10]i1p1f1	r[1-10]i1p1f1	
MIROC6 (50)	r[1-50]i1p1f1	r[1-50]i1p1f1	r[1-50]i1p1f1	
MIROC-ES2L (31)	r[1-30]i1p1f2 r1i1000p1f2	r[1-30]i1p1f2 r1i1000p1f2	r[1-30]i1p1f2 r1i1000p1f2	
MRI-ESM2-0 (12)	r[1-10]i1p1f1 r1i2p1f1 r1i1000p1f1	r[1-10]i1p1f1 r1i2p1f1 r1i1000p1f1	r[1-10]i1p1f1 r1i2p1f1 r1i1000p1f1	
GISS-E2-1-G (25)	r[1-10]i1p3f1 r[1-5]i1p1f3 r[1-4]i1p5f1 r[6-10]i1p5f1 r1i1p1f2	r[1-10]i1p3f1 r[1-5]i1p1f3 r[1-4]i1p5f1 r[6-10]i1p5f1 r1i1p1f2	r[1-10]i1p3f1 r[1-5]i1p1f3 r[1-4]i1p5f1 r[6-10]i1p5f1 r1i1p1f2	



GISS-E2-1-H (25)	r[1-10]i1p1f1 r[1-5]i1p1f2 r[1-5]i1p3f1 r[1-5]i1p5f1	r[1-10]i1p1f1 r[1-5]i1p1f2 r[1-5]i1p3f1 r[1-5]i1p5f1	r[1-10]i1p1f1 r[1-5]i1p1f2 r[1-5]i1p3f1 r[1-5]i1p5f1
GISS-E2-2-G (11)	r[1-6]i1p1f1 r[1-5]i1p3f1	r[1-6]i1p1f1 r[1-5]i1p3f1	r[1-6]i1p1f1 r[1-5]i1p3f1
Experiment ID	ssp126		
Variable	hurs	pr	sfcWind
Model (# of runs)	Variant Label	Variant Label	Variant Label
CESM2 (3)	r4i1p1f1 r10i1p1f1 r11i1p1f1	r4i1p1f1 r10i1p1f1 r11i1p1f1	r4i1p1f1 r10i1p1f1 r11i1p1f1
CESM2-WACCM (1)	r1i1p1f1	r1i1p1f1	r1i1p1f1
CNRM-ESM2-1 (5)	r[1-5]i1p1f2	r[1-5]i1p1f2	r[1-5]i1p1f2
GFDL-ESM4 (1)	r1i1p1f1	r1i1p1f1	r1i1p1f1
NorESM2-LM (1)	r1i1p1f1	r1i1p1f1	r1i1p1f1
UKESM1-0-LL (16)	r[1-12]i1p1f2 r[16-19]i1p1f2	r[1-12]i1p1f2 r[16-19]i1p1f2	r[1-12]i1p1f2 r[16-19]i1p1f2
INM-CM4-8 (1)	r1i1p1f1	r1i1p1f1	r1i1p1f1
INM-CM5-0 (1)	r1i1p1f1	r1i1p1f1	r1i1p1f1
MIROC6 (50)	r[1-50]i1p1f1	r[1-50]i1p1f1	r[1-50]i1p1f1
MIROC-ES2L (10)	r[1-10]i1p1f2	r[1-10]i1p1f2	r[1-10]i1p1f2
MRI-ESM2-0 (5)	r[1-5]i1p1f1	r[1-5]i1p1f1	r[1-5]i1p1f1
GISS-E2-1-G (16)	r[1-5]i1p1f2 r[1-5]i1p3f1 r[1-5]i1p5f1 r10i1p1f1	r[1-5]i1p1f2 r[1-5]i1p3f1 r[1-5]i1p5f1 r10i1p1f1	r[1-5]i1p1f2 r[1-5]i1p3f1 r[1-5]i1p5f1 r10i1p1f1
GISS-E2-1-H (10)	r[1-5]i1p1f2 r[1-5]i1p3f1	r[1-5]i1p1f2 r[1-5]i1p3f1	r[1-5]i1p1f2 r[1-5]i1p3f1
GISS-E2-2-G (5)	r[1-5]i1p3f1	r[1-5]i1p3f1	r[1-5]i1p3f1
Experiment ID	ssp245		
Variable	hurs	pr	sfcWind
Model (# of runs)	Variant Label	Variant Label	Variant Label
CESM2 (3)	r4i1p1f1 r10i1p1f1 r11i1p1f1	r4i1p1f1 r10i1p1f1 r11i1p1f1	r4i1p1f1 r10i1p1f1 r11i1p1f1
CESM2-WACCM (5)	r[1-5]i1p1f1	r[1-5]i1p1f1	r[1-5]i1p1f1
CNRM-ESM2-1	r[1-10]i1p1f2	r[1-10]i1p1f2	r[1-10]i1p1f2

(10)			
GFDL-ESM4 (1)	r1i1p1f1 <del>r[2-3]i1p1f1</del>	r1i1p1f1 <del>r[2-3]i1p1f1</del>	r1i1p1f1
NorESM2-LM (13)	r[1-3]i1p1f1 r[1-10]i1p1f2	r[1-3]i1p1f1 r[1-10]i1p1f2	r[1-3]i1p1f1 r[1-10]i1p1f2
UKESM1-0-LL (6)	r[1-4]i1p1f2 r8i1p1f2 r13i1p1f2	r[1-4]i1p1f2 r8i1p1f2 r13i1p1f2 <del>r[5-7]i1p1f2</del> <del>r[9-12]i1p1f2</del> <del>r[16-19]i1p1f2</del>	r[1-4]i1p1f2 r8i1p1f2 r13i1p1f2
INM-CM4-8 (1)	r1i1p1f1	r1i1p1f1	r1i1p1f1
INM-CM5-0 (1)	r1i1p1f1	r1i1p1f1	r1i1p1f1
MIROC6 (50)	r[1-50]i1p1f1	r[1-50]i1p1f1	r[1-50]i1p1f1
MIROC-ES2L (30)	r[1-30]i1p1f2	r[1-30]i1p1f2	r[1-30]i1p1f2
MRI-ESM2-0 (10)	r[1-5]i1p1f1 r[1-5]i3p1f1	r[1-5]i1p1f1 r[1-5]i3p1f1	r[1-5]i1p1f1 r[1-5]i3p1f1
GISS-E2-1-G (36)	r[1-10]i1p1f2 r[1-5]i1p3f1 r[1-10]i1p5f1 r[1-10]i1p5f2 r10i1p1f1	r[1-10]i1p1f2 r[1-5]i1p3f1 r[1-10]i1p5f1 r[1-10]i1p5f2 r10i1p1f1	r[1-10]i1p1f2 r[1-5]i1p3f1 r[1-10]i1p5f1 r[1-10]i1p5f2 r10i1p1f1
GISS-E2-1-H (10)	r[1-5]i1p1f2 r[1-5]i1p3f1	r[1-5]i1p1f2 r[1-5]i1p3f1	r[1-5]i1p1f2 r[1-5]i1p3f1
GISS-E2-2-G (5)	r[1-5]i1p3f1	r[1-5]i1p3f1	r[1-5]i1p3f1
Experiment ID	ssp370		
Variable	hurs	pr	sfcWind
Model (# of runs)	Variant Label	Variant Label	Variant Label
CESM2 (3)	r4i1p1f1 r[10-11]i1p1f1	r4i1p1f1 r[10-11]i1p1f1	r4i1p1f1 r[10-11]i1p1f1
CESM2-WACCM (3)	r[1-3]i1p1f1	r[1-3]i1p1f1	r[1-3]i1p1f1
CNRM-ESM2-1 (5)	r[1-5]i1p1f2	r[1-5]i1p1f2	r[1-5]i1p1f2
GFDL-ESM4 (1)	r1i1p1f1	r1i1p1f1	r1i1p1f1
NorESM2-LM (3)	r[1-3]i1p1f1	r[1-3]i1p1f1	r[1-3]i1p1f1
UKESM1-0-LL (10)	r[1-8]i1p1f2 r16i1p1f2 r19i1p1f2	r[1-8]i1p1f2 r16i1p1f2 r19i1p1f2	r[1-8]i1p1f2 r16i1p1f2 r19i1p1f2
INM-CM4-8 (1)	r1i1p1f1	r1i1p1f1	r1i1p1f1
INM-CM5-0 (5)	r[1-5]i1p1f1	r[1-5]i1p1f1	r[1-5]i1p1f1

MIROC6 (50)	r[1-50]i1p1f1	r[1-50]i1p1f1	r[1-50]i1p1f1
MIROC-ES2L (10)	r[1-10]i1p1f2	r[1-10]i1p1f2	r[1-10]i1p1f2
MRI-ESM2-0 (5)	r[1-5]i1p1f1	r[1-5]i1p1f1	r[1-5]i1p1f1
GISS-E2-1-G (27)	r[1-10]i1p1f2 r[1-4]i1p3f1 r[1-3]i1p3f2 r[1-10]i1p5f1	r[1-10]i1p1f2 r[1-4]i1p3f1 r[1-3]i1p3f2 r[1-10]i1p5f1	r[1-10]i1p1f2 r[1-4]i1p3f1 r[1-3]i1p3f2 r[1-10]i1p5f1
GISS-E2-1-H (6)	r[1-5]i1p1f2 r1i1p3f1	r[1-5]i1p1f2 r1i1p3f1	r[1-5]i1p1f2 r1i1p3f1
GISS-E2-2-G (5)	r[1-5]i1p3f1	r[1-5]i1p3f1	r[1-5]i1p3f1
Experiment ID	ssp585		
Variable	hurs	pr	sfcWind
Model (# of runs)	Variant Label	Variant Label	Variant Label
CESM2 (3)	r4i1p1f1 r10i1p1f1 r11i1p1f1	r4i1p1f1 r10i1p1f1 r11i1p1f1	r4i1p1f1 r10i1p1f1 r11i1p1f1
CESM2-WACCM (5)	r[1-5]i1p1f1	r[1-5]i1p1f1	r[1-5]i1p1f1
CNRM-ESM2-1 (5)	r[1-5]i1p1f1	r[1-5]i1p1f1	r[1-5]i1p1f1
GFDL-ESM4 (1)	r1i1p1f1	r1i1p1f1	r1i1p1f1
NorESM2-LM (1)	r1i1p1f1	r1i1p1f1	r1i1p1f1
UKESM1-0-LL (5)	r[1-4]i1p1f2 r8i1p1f2	r[1-4]i1p1f2 r8i1p1f2	r[1-4]i1p1f2 r8i1p1f2
INM-CM4-8 (1)	r1i1p1f1	r1i1p1f1	r1i1p1f1
INM-CM5-0 (1)	r1i1p1f1	r1i1p1f1	r1i1p1f1
MIROC6 (50)	r[1-50]i1p1f1	r[1-50]i1p1f1	r[1-50]i1p1f1
MIROC-ES2L (10)	r[1-10]i1p1f2	r[1-10]i1p1f2	r[1-10]i1p1f2
MRI-ESM2-0 (6)	r[1-5]i1p1f1 r1i2p1f1	r[1-5]i1p1f1 r1i2p1f1	r[1-5]i1p1f1 r1i2p1f1
GISS-E2-1-G (15)	r[1-5]i1p1f2 r[1-5]i1p3f1 r[1-5]i1p5f1	r[1-5]i1p1f2 r[1-5]i1p3f1 r[1-5]i1p5f1	r[1-5]i1p1f2 r[1-5]i1p3f1 r[1-5]i1p5f1
GISS-E2-1-H (10)	r[1-5]i1p1f2 r[1-5]i1p3f1	r[1-5]i1p1f2 r[1-5]i1p3f1	r[1-5]i1p1f2 r[1-5]i1p3f1
GISS-E2-2-G (5)	r[1-5]i1p3f1	r[1-5]i1p3f1	r[1-5]i1p3f1
Experiment ID	historical		
Variable	od550aer	od550dust	
Model (# of runs)	Variant Label	Variant Label	
CESM2 (11)	r[1-11]i1p1f1	r[1-11]i1p1f1	

CESM2-WACCM (3)	r[1-3]i1p1f1	r[1-3]i1p1f1
CNRM-ESM2-1 (9)	r[1-3]i1p1f2 r[4-5]i1p1f2 r[8-11]i1p1f2	r[1-3]i1p1f2 r[4-5]i1p1f2 r[8-11]i1p1f2
GFDL-ESM4 (1)	r1i1p1f1	r1i1p1f1
NorESM2-LM (1)	r1i1p1f1	r1i1p1f1
UKESM1-0-LL (19)	r[1-3]i1p1f2 r[4-19]i1p1f2	r[1-3]i1p1f2 r[4-19]i1p1f2
INM-CM4-8 (1)	r1i1p1f1	r1i1p1f1
INM-CM5-0 (10)	r[1-10]i1p1f1	r[1-10]i1p1f1
MIROC6 (10)	r[1-10]i1p1f1	r[1-10]i1p1f1
MIROC-ES2L (31)	r[1-30]i1p1f2 r1i1000p1f2	r[1-30]i1p1f2 r1i1000p1f2
MRI-ESM2-0 (12)	r[1-10]i1p1f1 r1i2p1f1 r1i1000p1f1	r[1-10]i1p1f1 r1i2p1f1 r1i1000p1f1
GISS-E2-1-G (19)	r[1-10]i1p3f1 r[1-4]i1p5f1 r[6-10]i1p5f1	r[1-10]i1p3f1
GISS-E2-1-H (10)	r[1-5]i1p3f1 r[1-5]i1p5f1	r[1-5]i1p3f1
GISS-E2-2-G (5)	r[1-5]i1p3f1	r[1-5]i1p3f1

**Table S2.** The normalized standard deviations and correlation coefficients for individual models shown in Fig. 1

Model	Dust concentrations		AOD	
	Normalized standard deviations	Correlation coefficient	Normalized standard deviations	Correlation coefficient
CESM2-WACCM	0.78	0.86	0.87	0.64
CESM2	0.74	0.87	0.89	0.6
CNRM-ESM2-1	0.44	0.85	0.28	0.79
GFDL-ESM4	0.54	0.81	0.59	0.58
GISS-E2-1-G	0.76	0.83	0.55	0.67
GISS-E2-1-H	0.62	0.83	0.51	0.66
GISS-E2-2-G	1.34	0.84	0.95	0.61
INM-CM4-8	0.11	0.49	0.42	0.44
INM-CM5-0	0.09	0.30	0.38	0.26
MIROC-ES2L	0.24	0.82	0.64	0.3
MIROC6	0.07	0.86	0.44	0.64
MRI-ESM2-0	2.16	0.86	0.82	0.33
NorESM2-LM	0.33	0.82	0.68	0.63
UKESM1-0-LL	1.03	0.88	0.36	0.75



**Table S3.** The summary of dust cycle at present day of selected models used in analysis<sup>a</sup>

Region	Model	Emission	Dry Deposition	Wet Deposition	Budget <sup>b</sup>
		Tg a <sup>-1</sup>	Tg a <sup>-1</sup>	Tg a <sup>-1</sup>	Tg a <sup>-1</sup>
Africa	CESM2-WACCM	1367	453	533	381
	CESM2	1349	448	517	383
	CNRM-ESM2-1	1931	1191	389	351
	GFDL-ESM4	1311	873	177	260
	GISS-E2-1-G	946	462	202	282
	GISS-E2-1-H	890	426	204	261
	GISS-E2-2-G	1327	814	125	388
	NorESM2-LM	1198	981	102	116
	UKESM1-0-LL	5289	4546	354	389
Asia	CESM2-WACCM	904	303	559	42
	CESM2	942	315	590	37
	CNRM-ESM2-1	487	308	224	-45
	GFDL-ESM4	720	519	230	-29
	GISS-E2-1-G	388	196	197	-5
	GISS-E2-1-H	382	189	197	-3
	GISS-E2-2-G	537	367	185	-14
	NorESM2-LM	549	447	123	-21
	UKESM1-0-LL	1937	1626	372	-61
Australia	CESM2-WACCM	53	14	23	16
	CESM2	78	21	33	25
	CNRM-ESM2-1	241	134	71	35
	GFDL-ESM4	155	88	23	43
	GISS-E2-1-G	41	19	12	11
	GISS-E2-1-H	41	18	12	11

	GISS-E2-2-G	61	35	9	17
	NorESM2-LM	35	25	5	5
	UKESM1-0-LL	814	703	77	34
South	CESM2-WACCM	10	10	46	-46
America	CESM2	11	11	48	-47
	CNRM-ESM2-1	18	15	14	-11
	GFDL-ESM4	355	215	93	48
	GISS-E2-1-G	16	14	38	-36
	GISS-E2-1-H	22	14	35	-27
	GISS-E2-2-G	23	25	54	-56
	NorESM2-LM	10	9	11	-10
	UKESM1-0-LL	36	42	42	-48
North	CESM2-WACCM	2	25	78	-100
America	CESM2	2	26	77	-101
	CNRM-ESM2-1	3	51	34	-82
	GFDL-ESM4	46	69	59	-81
	GISS-E2-1-G	2	24	63	-85
	GISS-E2-1-H	1	20	56	-75
	GISS-E2-2-G	2	52	74	-124
	NorESM2-LM	2	14	16	-28
	UKESM1-0-LL	82	117	72	-107
Europe	CESM2-WACCM	2	20	65	-83
	CESM2	2	22	69	-88
	CNRM-ESM2-1	2	12	52	-63
	GFDL-ESM4	7	18	42	-53
	GISS-E2-1-G	4	8	44	-48
	GISS-E2-1-H	5	9	42	-46
	GISS-E2-2-G	5	15	36	-46
	NorESM2-LM	9	16	14	-21

	UKESM1-0-LL	10	18	40	-48
Pacific	CESM2-WACCM		6	46	-52
Ocean	CESM2		7	53	-60
	CNRM-ESM2-1		8	13	-21
	GFDL-ESM4		41	72	-113
	GISS-E2-1-G	/	9	44	-53
	GISS-E2-1-H		9	40	-49
	GISS-E2-2-G		29	86	-115
	NorESM2-LM		4	14	-19
	UKESM1-0-LL		11	67	-78
Indian	CESM2-WACCM		33	126	-160
Ocean	CESM2		36	131	-167
	CNRM-ESM2-1		72	72	-144
	GFDL-ESM4		71	70	-141
	GISS-E2-1-G	/	19	39	-57
	GISS-E2-1-H		20	44	-64
	GISS-E2-2-G		37	37	-74
	NorESM2-LM		41	30	-70
	UKESM1-0-LL		87	91	-178
Atlantic	CESM2-WACCM		68	243	-311
Ocean	CESM2		70	243	-313
	CNRM-ESM2-1		162	124	-285
	GFDL-ESM4		133	162	-295
	GISS-E2-1-G	/	54	146	-200
	GISS-E2-1-H		47	141	-188
	GISS-E2-2-G		106	121	-227
	NorESM2-LM		79	51	-130
	UKESM1-0-LL		139	163	-302
Arctic	CESM2-WACCM	/	0.4	4	-5

Ocean	CESM2	0.5	4	-5
	CNRM-ESM2-1	0.5	1	-1
	GFDL-ESM4	0.4	3	-3
	GISS-E2-1-G	0.3	2	-2
	GISS-E2-1-H	0.2	2	-2
	GISS-E2-2-G	1.4	3	-5
	NorESM2-LM	0.1	1	-1
	UKESM1-0-LL	0.2	2	-2

---

<sup>a</sup> Please notice that the median values in Table 3 are derived as the regional total of gridded median results from CMIP6 models, and are different from the median values of the regional total from CMIP6 models shown above.

<sup>b</sup> Budget = Emission - Dry Deposition - Wet Deposition

**Table S4.** Multi-model ensemble projection of absolute (Gg) and relative changes (%) in dust column load by the end of 21<sup>st</sup> century (2090-2099)

Region*/ Scenario	SSP126		SSP245		SSP370		SSP585	
	Absolute	Relative	Absolute	Relative	Absolute	Relative	Absolute	Relative
NAF	77.2±274.1	1.6	217.3±293.7	4.4	162.5±325.7	3.3	668.3±458.1	13.5
TGD	-3.9±60.0	-0.6	-26.1±162.6	-4.0	-54.7±195.9	-8.3	-43.6±199.5	-6.6
MEWA	-37.2±229.3	-1.5	-61.5±335.0	-2.5	-130.4±414.0	-5.3	64.2±503.4	2.6
AUS	10.7±55.0	4.5	28.9±66.6	12.3	22.3±77.0	9.5	65.8±84.6	28.0
NAM	0.5±17.3	3.4	0.1±19.0	1.1	0.1±20.0	1.0	0.8±20.9	5.7
SAM	2.9±97.9	10.1	3.8±124.9	13.4	1.6±87.6	5.5	1.3±75.0	4.7
SAF	1.3±19.9	2.2	7.5±25.5	13.3	21.6±113.0	38.3	10.2±62.8	18.0
SAS	11.4±96.2	1.9	-13.9±86.0	-2.3	-42.2±105.3	-6.9	7.6±134.5	1.3
EAS	-4.0±52.2	-1.3	-6.3±63.1	-2.0	-32.6±75.2	-10.5	-20.6±79.6	-6.6

\* The domain of each region is shown in Fig. 4a and Fig. 8a.



**Table S5.** Multi-model ensemble projection of the absolute ( $\text{Tg a}^{-1}$ ) and relative changes (%) in dust emissions by the end of this century (2090-2099) at vegetation-free grid points

Region*	SSP1-2.6		SSP2-4.5		SSP3-7.0		SSP5-8.5	
	Absolute	Relative	Absolute	Relative	Absolute	Relative	Absolute	Relative
NAF	10.1±121.7	1.2	5.8±131.5	0.7	4.2±174.1	0.5	47.4±178.9	5.6
TGD	-0.4±23.5	-0.8	-2.5±41.3	-4.9	-6.2±53.6	-11.9	-4.6±55.7	-8.9
MEWA	-0.7±43.1	-0.3	-4.5±66.4	-1.8	-4.4±81.0	-1.8	6.8±87.2	2.7
AUS	1.2±16.9	2.9	2.0±20.5	5.1	-0.1±47.2	-0.3	4.3±51.6	10.7
NAM	0.03±4.7	2.2	0.02±6.1	1.3	0.01±5.4	0.8	0.02±5.7	1.4
SAM	0.01±32.3	0.2	0.4±42.1	6.7	-0.1±31.2	-2.1	-0.4±27.7	-6.2
SAF	0.2±4.1	2.3	0.5±4.1	6.1	0.7±10.6	9.0	0.9±5.0	11.4

\* The domain of each region is shown in Fig. 4a

**Table S6.** Multi-model ensemble projection of the absolute ( $\text{Tg a}^{-1}$ ) and relative changes (%) in dust emissions by the end of this century (2090-2099) using all 14 CMIP6 models

Region*	SSP1-2.6		SSP2-4.5		SSP3-7.0		SSP5-8.5	
	Absolute	Relative	Absolute	Relative	Absolute	Relative	Absolute	Relative
	median $\pm$ SD		median $\pm$ SD		median $\pm$ SD		median $\pm$ SD	
NAF	10.3 $\pm$ 131.5	1.4	15.8 $\pm$ 159.9	2.2	19.5 $\pm$ 181.6	2.7	48.0 $\pm$ 215.2	6.6
TGD	0.6 $\pm$ 32.3	1.1	-1.4 $\pm$ 37.9	-2.9	-4.8 $\pm$ 50.6	-9.6	-3.5 $\pm$ 54.0	-6.9
MEWA	1.8 $\pm$ 68.4	0.9	0.6 $\pm$ 69.7	0.3	-1.7 $\pm$ 68.1	-0.8	5.6 $\pm$ 93.8	2.8
AUS	-0.6 $\pm$ 15.5	-1.3	0.2 $\pm$ 26.5	0.4	-0.3 $\pm$ 49.4	-0.7	1.9 $\pm$ 52.7	4.3
NAM	0.03 $\pm$ 3.9	1.8	0.02 $\pm$ 5.2	1.3	0.02 $\pm$ 5.4	1.6	0.04 $\pm$ 6.3	2.6
SAM	0.4 $\pm$ 30.6	5.0	0.6 $\pm$ 47.6	7.2	0.2 $\pm$ 58.6	1.9	0.1 $\pm$ 84.5	0.9
SAF	0.02 $\pm$ 4.6	0.2	0.7 $\pm$ 5.2	7.8	1.3 $\pm$ 10.2	13.8	1.5 $\pm$ 7.8	15.9

\* The domain of each region is shown in Fig. 4a

**Table S7.** The information of all available CMIP6 models for climate projection

Model	Resolution	Model	Resolution	Model	Resolution
ACCESS-CM2	1.875°×1.24°	EC-Earth3-Veg-LR	1.125°×1.125°	MPI-ESM1-2-LR	1.875°×1.875°
ACCESS-ESM1-5	1.875°×1.24°	FGOALS-f3-L	1°×1°	MRI-ESM2-0	1.125°×1.125°
AWI-CM-1-1-MR	0.94°×0.94°	FGOALS-g3	2°×2°	NorESM2-LM	2.5°×1.875°
BCC-CSM2-MR	1.125°×1.125°	GFDL-ESM4	1°×1°	NorESM2-MM	1.91°×0.94°
CAMS-CSM1-0	1.125°×1.125°	IITM-ESM	1.875°×1.91°	TaiESM1	1.25°×0.94°
CAS-ESM2-0	1.4°×1.4°	INM-CM4-8	2°×1.5°	CNRM-CM6-1	0.5°×0.5°
CESM2-WACCM	1.25°×0.94°	INM-CM5-0	2°×1.5°	CNRM-CM6-1-HR	0.5°×0.5°
CMCC-CM2-SR5	1.25°×0.94°	IPSL-CM6A-LR	2.5°×1.26°	CNRM-ESM2-1	1.4°×1.4°
CMCC-ESM2	1.25°×0.94°	KACE-1-0-G	1.875°×1.25°	MIROC-ES2L	2.8°×2.8°
CanESM5	2.8°×2.8°	MIROC6	1.4°×1.4°	UKESM1-0-LL	1.875°×1.25°
EC-Earth3	0.7°×0.7°	MPI-ESM1-2-HR	0.94°×0.94°	/	/